BIOCHEMISTRY
including biophysical chemistry & molecular biology

Article

pubs.acs.org/biochemistry

Functional Roles of D2-Lys317 and the Interacting Chloride Ion in the Water Oxidation Reaction of Photosystem II As Revealed by Fourier Transform Infrared Analysis

Hiroyuki Suzuki,[†] Jianfeng Yu,[‡] Takashi Kobayashi,[†] Hanayo Nakanishi,[†] Peter J. Nixon,[‡] and Takumi Noguchi*,[†]

[†]Division of Material Science, Graduate School of Science, Nagoya University, Furo-cho, Chikusa-ku, Nagoya 464-8602, Japan
[‡]Department of Life Sciences, Imperial College London, South Kensington Campus, London SW7 2AZ, United Kingdom

Supporting Information

ABSTRACT: Photosynthetic water oxidation in plants and cyanobacteria is catalyzed by a Mn_4CaO_5 cluster within the photosystem II (PSII) protein complex. Two Cl^- ions bound near the Mn_4CaO_5 cluster act as indispensable cofactors, but their functional roles remain to be clarified. We have investigated the role of the Cl^- ion interacting with D2-K317 (designated Cl-1) by Fourier transform infrared spectroscopy (FTIR) analysis of the D2-K317R mutant of *Synechocystis* sp. PCC 6803 in combination with Cl^-/NO_3^- replacement. The D2-K317R mutation perturbed the bands in the regions of the COO^- stretching and backbone amide vibrations in the FTIR difference spectrum upon the $S_1 \rightarrow S_2$ transition. In addition, this mutation altered the ^{15}N isotope-edited NO_3^- bands in the spectrum of NO_3^--treated PSII. These results provide the first experimental evidence that the Cl-1 site is coupled with the Mn_4CaO_5 cluster and its interaction is affected by the $S_1 \rightarrow S_2$ transition. It was also shown that a negative band at 1748 cm^{-1} arising from COOH group(s) was altered to a positive intensity by the D2-K317R mutation as well as by NO_3^- treatment, suggesting that the Cl-1 site affects the pK_a of COOH/COO^- group(s) near the Mn_4CaO_5 cluster in a common hydrogen bond network. Together with the observation that the efficiency of the $S_3 \rightarrow S_0$ transition significantly decreased in the core complexes of D2-K317R upon moderate dehydration, it is suggested that D2-K317 and Cl-1 are involved in a proton transfer pathway from the Mn_4CaO_5 cluster to the lumen, which functions in the $S_3 \rightarrow S_0$ transition.

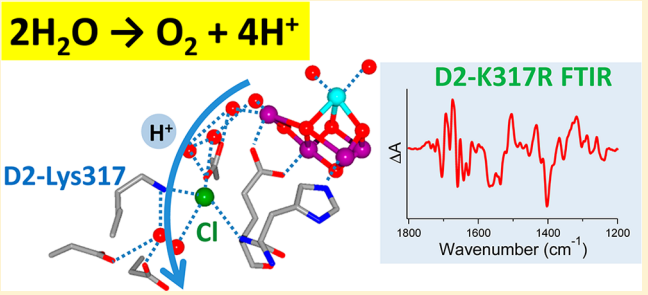

Photosynthesis is the biological process by which light energy is converted to chemical energy through the formation of sugars from CO_2. Plants and cyanobacteria utilize water, which is present in abundance on earth, as the ultimate electron donor to reduce CO_2. Oxidation of water liberates molecular oxygen, which is the source of the earth's oxygenic atmosphere. Thus, oxygenic photosynthesis sustains life on earth as both an energy source and an oxygen source.

The water oxidation reactions take place in photosystem II (PSII) protein complexes embedded in thylakoid membranes.[1−6] The catalytic site of water oxidation is the water oxidizing center (WOC), which consists of a Mn_4CaO_5 cluster and surrounding amino acid ligands (six carboxylate groups and one imidazole group belonging to the D1 and CP43 subunits).[7−10] Water oxidation proceeds through a cycle of five intermediates designated S_n states (n = 0−4),[1−6] with a larger value of n implying a higher oxidation state of the Mn_4CaO_5 cluster. Among them, the S_1 state is the most stable in the dark, and the S_n state (n = 0−3) advances to the next S_{n+1} state upon one-electron abstraction by a chlorophyll cation, $P680^+$, which is produced by light-induced charge separation, via the redox-active tyrosine Y_Z. The S_4 state is a transient state that immediately relaxes to the S_0 state releasing O_2.

Chloride has long been known to be an indispensable cofactor for water oxidation.[11−14] Upon Cl^- depletion, S-state transitions beyond the S_2 state are blocked and O_2 evolution is inhibited.[15−17] O_2 evolution can still occur when Cl^- is replaced by monovalent anions such as Br^-, NO_3^-, and I^-,[18,19] but at a lower rate. Upon these substitutions for Cl^-, the $S_3 \rightarrow S_0$ transition is mainly retarded.[18,19] It has been suggested that two types of Cl^- with high and low affinities are involved in water oxidation.[20−22] Indeed, X-ray crystallographic studies of PSII from the thermophilic cyanobacteria *Thermosynechococcus elongatus* and *Thermosynechococcus vulcanus* showed two binding sites for Br^- or I^- near the Mn_4CaO_5 cluster upon replacement of Cl^-.[23,24] The recent high-resolution (1.9 Å) X-ray structure of PSII from *T. vulcanus* confirmed that one Cl^- ion is indeed bound to each of these sites.[9] One of these Cl^- ions (Cl-1) is located 6.6 Å from Mn4 and is surrounded by the

Received: December 24, 2012
Revised: June 16, 2013
Published: June 20, 2013

   dx.doi.org/10.1021/bi301699h | *Biochemistry* 2013, 52, 4748−4757

side chains of D2-K317 and D1-N181, the backbone NH group of D1-E333, and two water molecules, while the other Cl^- (Cl-2) is located 7.4 Å from Mn2 and surrounded by the backbone NH groups of CP43-E354, D1-N338, and D1-F339 and two water molecules (Figure 1). However, another X-ray study (at

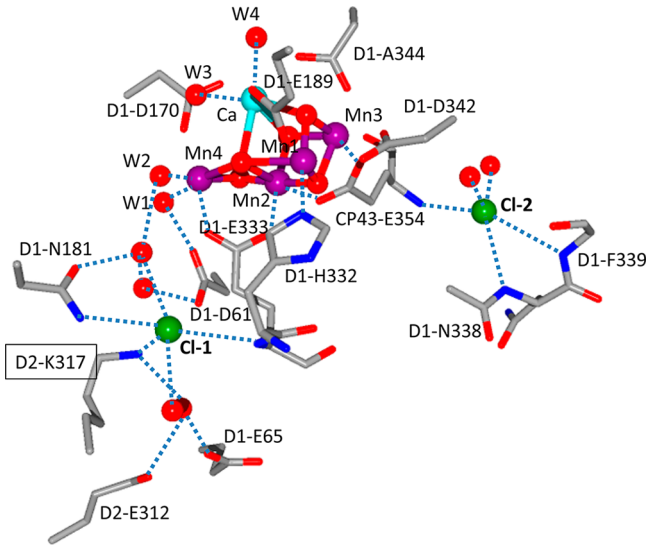

Figure 1. Structure around the Mn_4CaO_5 cluster and two Cl^- ions deduced from the X-ray crystal structure of photosystem II at 1.9 Å resolution[9] (Protein Data Bank entry 3ARC). Amino acid side chains, backbone amides, and water molecules, which directly interact with the Mn cluster and Cl ions or are involved in a hydrogen bond network, are shown.

2.9 Å resolution) of *T. elongatus* PSII showed only one Cl^- at the Cl-1 site,[8] and furthermore, PSII treated with the herbicide terbutryn contained in addition to the Cl-1 site (designated Cl-1A), a second Cl^--binding site (Cl-1B) near Cl-1A.[25] Thus, there are possibilities that the Cl^--binding sites are dependent on PSII preparations or even that Cl^- changes its binding site during the S-state cycle.[25]

Because Cl-1 and Cl-2 interact with the backbone amides of ligands to the Mn_4CaO_5 cluster, at D1-E333 and D1-H332 for Cl-1 and at CP43-E354 for Cl-2, it has been proposed that Cl^- functions to maintain the structure of the Mn_4CaO_5 cluster.[24] In addition, because Cl-1 is located close to the entrance of a possible proton channel, Cl-1 has been proposed to have a function of forming a proton pathway from the Mn_4CaO_5 cluster to the lumen.[8,23,24] Recent molecular dynamics and Monte Carlo simulations have proposed that one role for Cl^- might be to prevent the formation of a salt bridge between D2-K317 and D1-D61 that could suppress proton transfer.[26] Also, kinetic measurements of Ca^{2+}/Sr^{2+}- and Cl^-/I^--exchanged PSII showed significant retardation of the $S_3Y_Z^{\bullet} \rightarrow (S_3Y_Z^{\bullet})' \rightarrow S_0$ kinetics in PSII containing bound Sr^{2+} and I^-, suggesting that the Ca^{2+} and Cl^- sites are connected though a hydrogen bond network that acts as a channel for proton release.[19] It was further proposed that proton transfer is promoted by the movement of Cl^- between the Cl-1A and Cl-1B sites.[25] However, there is still a lack of evidence for the functional roles of Cl^- at each of the binding sites. Light-induced Fourier transform infrared (FTIR) difference spectroscopy is a powerful method for examining the detailed molecular structures and reactions of the WOC during water oxidation.[27−31] Structural information about the Mn cluster,[32] amino acid side chains,[33−38] protein main chains,[39] and water molecules[40,41] coupled to the S-state transitions has been obtained. Hasegawa et al.[42] previously detected S_2-minus-S_1 (hereafter designated S_2/S_1) FTIR difference spectra of PSII preparations in which Cl^- is replaced with various monovalent anions. Substitution with Br^-, I^-, and NO_3^-, which supported O_2 evolution, restored the overall features of the spectrum, whereas Cl^- depletion and replacement with F^- and acetate, which suppressed O_2 evolution, induced significant structural changes in the carboxylate and amide regions. They further identified the NO stretching bands of NO_3^- in the S_2/S_1 spectrum of Cl^-/NO_3^--replaced PSII using isotope-labeled NO_3^- ($^{15}NO_3^-$ or $N^{16}O_3^-$) and discussed the structure of NO_3^- at the Cl^- site.[42,43] However, in light of the information from the recent X-ray structures that suggested two Cl^- sites probably exist around the Mn_4CaO_5 cluster,[8,9,23,24] the questions of which Cl^- site the NO_3^- ion binds and whether both of them have been detected by FTIR arise. These questions are essential for the investigation of the role of Cl^- in the water oxidation mechanism using NO_3^- substitution.

In this study, we have used light-induced FTIR difference spectroscopy to investigate the functional role of Cl^- bound to the Cl-1 site through analysis of mutant PSII complexes isolated from the cyanobacterium *Synechocystis* sp. PCC 6803 in which D2-K317, which directly interacts with Cl-1, is replaced with Arg. In addition, we monitored the vibrations of NO_3^-, which was substituted for Cl^-, and examined the effect of the D2-K317R mutation to study the interaction of NO_3^- in the Cl-1 site. The obtained data revealed that the strong structural coupling exists between the Cl-1 site and the Mn_4CaO_5 cluster and support a model in which D2-K317 and Cl-1 are involved in a proton transfer pathway in the $S_3 \rightarrow S_0$ transition.

MATERIALS AND METHODS

Construction of Mutants. The D2-K317R mutant and WT control strain were constructed according to the method of Tang et al.[44] except that the recipient strain Tol145/CP47-His, obtained by transforming strain Tol145[44] with genomic DNA from strain PSII-His,[45] also encoded a C-terminal His-tagged derivative of CP47. Plasmid pDC074 was used as the parental vector for site-directed mutagenesis.[44] Mutations were introduced into the plasmid by overlap extension polymerase chain reaction (PCR), so that the AAA codon specifying D2-K317 was replaced with the AGA codon (to make D2-K317R). A silent mutation was also introduced at F311 (TTT to TTC) to create an *Eco*RI site to allow detection of mutants. A WT control strain was generated using the pDC074 plasmid. The genotypes of the cyanobacterial strains were confirmed by PCR analysis and DNA sequencing.

Cell Growth and Isolation of His-Tagged PSII Oxygen-Evolving Complexes. Cells were maintained on BG-11 plates containing 5 mM glucose, 25 mg/L kanamycin, 15 mg/L erythromycin, and 10 μM DCMU.[44] Oxygen-evolving His-tagged PSII complexes were isolated from 30 L cultures using the procedure described by Service et al.[36] The presence of the engineered mutations in the final culture was verified by PCR and DNA sequencing. The rates of light-saturated oxygen evolution determined in the presence of 50 mM MES-NaOH (pH 6.5), 500 mM sucrose, 30 mM $CaCl_2$, 10 mM $MgCl_2$, and electron acceptors 1 mM potassium ferricyanide and 0.1 mM 2,6-dichloro-1,4-benzoquinone (DCBQ) were in the range of 2000−2900 μmol of O_2 (mg of Chl)$^{-1}$ h^{-1} for both the WT and mutant complexes, in line with previous values obtained

dx.doi.org/10.1021/bi301699h | *Biochemistry* 2013, 52, 4748−4757

with His-tagged[46] and untagged WT PSII complexes.[47,48] In particular, this O_2 evolution activity of WT is similar to that reported by Pokhrel et al.,[49] although higher values have been reported by Debus and colleagues.[36] It should be noted that our assay buffer contains sufficient calcium (30 mM) to maintain O_2 evolution. Even in the absence of calcium in the buffer, the O_2 evolution activity of the PSII core complexes from *Synechocystis* sp. PCC 6803 is decreased only by 25−45%.[49] Growth experiments were performed by measuring the OD_{730} of liquid BG-11 cultures inoculated to an initial cell density with an OD_{730} of 0.01. Four 30 mL cultures were grown for each strain in Corning cell culture flasks (25 cm^2, canted neck, vente) at 29 °C at a constant irradiance of 40 $\mu E\ m^{-2}\ s^{-1}$ fluorescent white light and at 100 rpm. Chloride depletion was performed by replacing all chloride salts in the medium with their nitrate equivalents.

For examination of the Cl^- concentration dependence of the O_2 evolution activity, O_2 evolution of the PSII core complexes was measured in an assay buffer containing 500 mM sucrose, 120 mM MES-NaOH (pH 6.5), 30 mM $Ca(OH)_2$, and 10 mM $Mg(OH)_2$ together with 0.0, 2.5, 5.0, 10, 20, or 40 mM NaCl, in the presence of 0.5 mM DCBQ as an electron acceptor. The lowest Cl^- concentration was 0.6 mM because of the Cl^- contamination from the original buffer [50 mM Mes-NaOH (pH 6.0), 1.2 M betaine, 20 mM $CaCl_2$, 10 mM $MgCl_2$, 25% glycerol, 100 mM histidine hydrochloride, and 0.04% *n*-dodecyl *β*-D-maltoside (DM)], in which the PSII core complexes were suspended.

FTIR Measurements. The PSII complexes were suspended in a 10 mM Mes-NaOH (pH 6.0) buffer containing 5 mM NaCl, 5 mM $CaCl_2$, 40 mM sucrose, and 0.06% *n*-dodecyl *β*-D-maltoside (DM) and concentrated to ∼2.25 mg of Chl/mL using Microcon-100 (Amicon). In the experiments that aimed to study the effect of NO_3^- replacement for Cl^-, the core complexes were first treated with NO_3^- in a 20 mM Mes-NaOH buffer (pH 6.0) containing 100 mM $NaNO_3$, 5 mM $Ca(OH)_2$, 40 mM sucrose, and 0.06% DM. The sample was then washed with a buffer with the same content except for 10 mM $NaNO_3$ and was concentrated to ∼2.5 mg of Chl/mL. An aliquot of the sample suspension (10 μL) in the buffer with Cl^- or NO_3^- was mixed with 1 μL of 100 mM potassium ferricyanide and dried on a CaF_2 plate (25 mm × 25 mm) under N_2 gas in an oval shape (6 mm × 9 mm). The sample was hydrated by placing 2 μL of a 40% (v/v) glycerol/water solution in a sealed IR cell without touching the sample.[50] For solution measurements, the dried sample was resuspended with 0.8 μL of water and sandwiched with another CaF_2 plate with a circular groove (10 mm inner diameter, 1 mm width) as described previously.[51] The sample temperature was kept at 10 °C by circulating cold water through a copper holder.

Flash-induced FTIR difference spectra were measured on a Bruker IFS-66/S spectrophotometer equipped with an MCT detector (InfraRed D316/8) at 4 cm^{-1} resolution.[29] Flash illumination was performed by a Q-switched Nd:YAG laser (Quanta-Ray GCR-130, 532 nm, ∼7 ns full width at half-maximum) with a power of ∼7 mJ cm^{-1} $pulse^{-1}$ at the sample point. For the measurements of S_2/S_1 FTIR difference spectra, the sample was first illuminated by two preflashes (1 s interval) followed by dark adaptation for 10 min. A single-beam spectrum (100 scans, 50 s scan) was recorded twice before illumination of a single flash and once after the illumination, and then the sample was adapted to the dark for 10 min. This process of measurement and dark adaptation was repeated 48 and 24 times for WT and D2-K317R, respectively, and the spectra were averaged to calculate the S_2/S_1 and dark/dark (noise level) spectra (the diagram of the measurement procedure is shown in Figure S1 of the Supporting Information). Spectra were measured using two different samples to obtain final average data.

A similar measurement scheme was used for the PSII sample treated with NO_3^-. In this case, the dark incubation time was 5 min and single-beam spectra were recorded by 20 s scans reflecting faster S_2 relaxation with NO_3^- ($\tau \sim 200$ and 100 s with Cl^- and NO_3^-, respectively, under our measurement conditions). The cycle was repeated 168 times, and the data were averaged to calculate S_2/S_1 difference spectra.

For the measurements of FTIR difference spectra of the S-state cycle, after two preflashes followed by dark adaptation for 15 min, four flashes were applied with 10 s intervals. Single-beam spectra (20 scans, 10 s scan) were measured before, between, and after the flashes. The sample was then adapted to the dark for 15 min; this entire cycle was repeated 17 or 18 times, and the data were averaged to calculate the difference spectra upon first, second, third, and fourth flash illumination (the details of the measurement procedure are shown in the diagram in Figure S1 of the Supporting Information).

When double difference spectra were calculated, factors for subtraction were determined to minimize the least-squares of the double difference between 1470 and 1270 cm^{-1} representing the symmetric COO^- region. The spectral analysis was performed using Igor Pro (WaveMetrics Inc.).

RESULTS

The D2-K317R mutant and its WT control strain were constructed in the phycocyanin-deficient "olive" strain of *Synechocystis* sp. PCC 6803, which contains approximately twice as much PSII as the widely used glucose-tolerant strain.[52] Both D2-K317R and the WT control strain also expressed a C-terminal His-tagged derivative of CP47 to allow isolation of His-tagged PSII complexes. The D2-K317R mutant retained the ability to grow photoautotrophically at rates similar to that of the WT control in both liquid BG-11 medium and BG-11 medium that had been depleted of chloride (Figure S2 of the Supporting Information). Oxygen evolution in young cultures grown mixotrophically in the presence of 5 mM glucose to a concentratioon of 1−2 μg of chlorophyll/mL was also experimentally indistinguishable from that of the WT control strain, with both giving light-saturated rates of 530−600 μmol of O_2 (mg of Chl)$^{-1}$ h^{-1} in the presence of the electron acceptors 0.1 mM DCBQ and 1 mM potassium ferricyanide. These data therefore suggest that the conservative replacement of D2-K317 with Arg does not have drastic effects on PSII activity *in vivo* under the experimental conditions used.

Figure 2a shows an S_2/S_1 FTIR difference spectrum in the typical protein region (1800−1200 cm^{-1}) of a hydrated film of His-tagged oxygen-evolving PSII core complexes isolated from the WT control strain of *Synechocystis* sp. PCC 6803. The spectral features were very similar to those reported previously for PSII complexes from the same species[34−38] as well as from *T. elongatus*.[40,41] Bands at 1450−1300 cm^{-1} have been assigned to the symmetric COO^- stretching vibrations of carboxylate residues, while asymmetric COO^- bands appear at 1600−1500 cm^{-1}.[53,54] The strong features in these regions indicate that the several carboxylate groups are coupled to the structural changes in the $S_1 \rightarrow S_2$ transition. The features in the 1700−1600 cm^{-1} region are mainly attributed to the amide I bands (C═O

dx.doi.org/10.1021/bi301699h | *Biochemistry* 2013, 52, 4748−4757

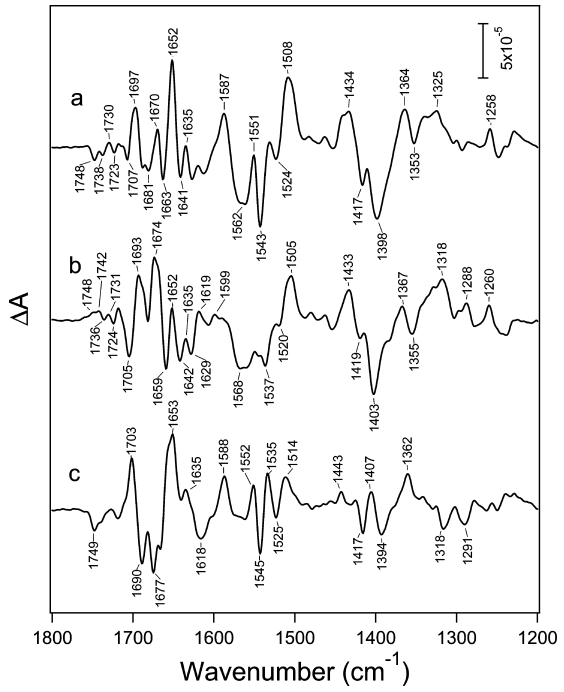

Figure 2. Flash-induced S_2/S_1 FTIR difference spectra in the 1800−1200 cm^{-1} region of moderately hydrated films of the PSII complexes from WT (a) and the D2-K317R mutant (b) of *Synechocystis* sp. PCC6803, and (c) their double difference spectrum (a minus b).

stretches of backbone amides), representing the conformational changes of proteins around the WOC.[53,54] Amide II bands (NH bends and CN stretches of backbone amides) that are coupled to amide I bands appear around 1550 cm^{-1}, superimposing with the asymmetric COO^- bands.[53,54] Recently, it was shown that the CN/NH_2 vibrations of a guanidinium group most probably from CP43-Arg357 are present at 1700−1600 cm^{-1}.[38] The negative band at 1748 cm^{-1} has been assigned to the C═O stretching vibration(s) of a COOH group(s) in the hydrogen bond network around the Mn_4CaO_5 cluster.[55]

Figure 2b shows the S_2/S_1 difference spectrum of a hydrated film of PSII from the D2-K317R mutant. The spectral features are clearly different from those of the WT spectrum, although the signal intensities were basically identical, consistent with the similar O_2 evolution activities. In the symmetric COO^- stretching region (1450−1300 cm^{-1}), the most prominent negative band at 1398 cm^{-1} is upshifted to 1403 cm^{-1} with a sharper bandwidth, while the positive and negative peaks at 1364 and 1417 cm^{-1}, respectively, are slightly upshifted to 1367 and 1419 cm^{-1}, respectively, with weakened intensities. In the asymmetric COO^-/amide II region (1600−1500 cm^{-1}), the intensities of positive peak at 1587 cm^{-1} and the negative peaks at 1543 and 1524 cm^{-1} were significantly weakened in the K317R mutant. In the amide I region (1700−1600 cm^{-1}), the band pattern significantly changed: a new peak appeared at 1619 cm^{-1}, and the positive peaks at 1652 and 1670 cm^{-1} became smaller and stronger, respectively. The CN/NH_2 bands of Arg, which was introduced by the K317R mutation, could be involved in this region. The negative band at 1748 cm^{-1} due to a COOH group(s) was changed to a positive feature with peaks at 1748 and 1742 cm^{-1}. The negative peak at 1705 cm^{-1} could be the signal of Y_D[56,57] or Y_Z[58] in some inactive centers.

These spectral differences are better expressed in the WT-minus-K317R double difference spectrum (Figure 2c). As expected, prominent features are observed in the symmetric COO^- regions with positive peaks at 1443, 1407, and 1362 cm^{-1} and negative peaks at 1417 and 1394 cm^{-1}. Also, large features were observed in the amide I and amide II/asymmetric COO^- regions. Positive peaks at 1703, 1653, 1635, 1588, 1552, 1535, and 1514 cm^{-1} and negative peaks at 1690, 1677, 1618, 1545, and 1525 cm^{-1} were observed. The COOH band was detected as a negative peak at 1749 cm^{-1}.

Figure 3 (red line) shows the S_2/S_1 FTIR difference spectra of NO_3^--treated core complexes of WT (a) and D2-K317R (b)

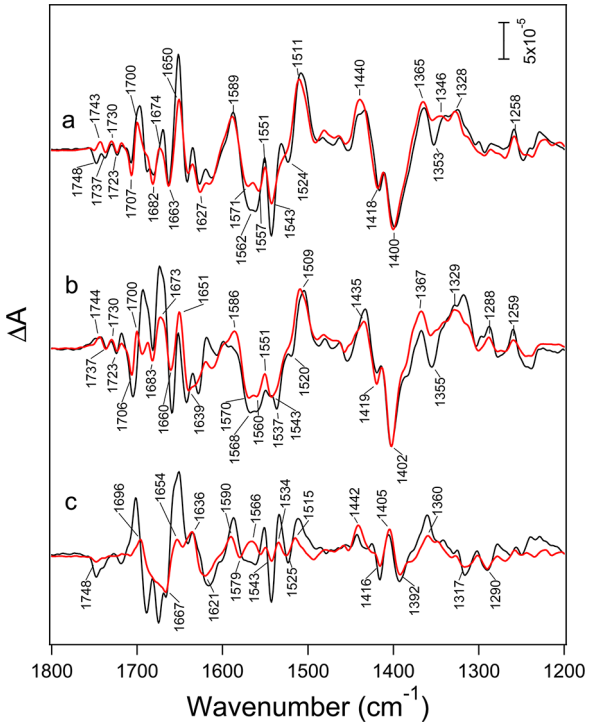

Figure 3. Flash-induced S_2/S_1 FTIR difference spectra of NO_3^--treated PSII complexes (red lines) from WT (a) and D2-K317R (b), and (c) their double difference spectrum (a minus b) in comparison with the corresponding spectra of untreated PSII (black lines, identical to Figure 2).

in comparison with the corresponding spectra of untreated PSII (black lines; identical to parts a and b of Figure 2, respectively). The overall features were very similar between the untreated and NO_3^--treated PSII in both WT and K317R, but some differences were also observed. (1) A negative dip at 1355−1353 cm^{-1} almost disappeared by the overlap of the positive intensity in this region. (2) In the amide II region, the intensities of the negative bands at 1562, 1543, and 1524 cm^{-1} in WT and 1568, 1537, and 1520 cm^{-1} in K317R became weaker. (3) The intensities of the peaks in the amide I region (1700−1600 cm^{-1}) were generally weakened. (4) In WT, the negative peak at 1748 cm^{-1} was changed to a positive peak at 1743 cm^{-1}, whereas in D2-K317R, no prominent change was observed at this position.

In Figure 3c, a WT-minus-K317R double difference spectrum of the NO_3^--treated PSII (red line) is compared with that of the untreated PSII (black line, identical to Figure 2c). The spectral features in the symmetric COO^- region (1450−1300 cm^{-1}) were very similar, reflecting similar

dx.doi.org/10.1021/bi301699h | *Biochemistry* 2013, 52, 4748−4757

structural changes in the carboxylate groups even after NO_3^- treatment. In contrast, the band intensities were much smaller in the amide I and II regions, although the overall features and band positions were similar. The latter observation, however, should be carefully interpreted because the amide I and II bands of protein main chains are generally sensitive to subtle differences in sample conditions.

It has previously been shown that the asymmetric NO stretching vibrations of NO_3^- bound near the Mn_4CaO_5 cluster exhibit bands only in the 1450−1250 cm^{-1} region.[42,43] Thus, the NO_3^--induced spectral changes near 1350 cm^{-1} mentioned above should involve the bands of NO_3^-. To identify the NO_3^- bands in the S_2/S_1 difference spectra and examine the effect of the D2-K317R mutation on the NO_3^- bands, the S_2/S_1 spectra of PSII treated with isotope-labeled $^{15}NO_3^-$ were measured for WT and D2-K317R. Figure 4 compares the spectra in the

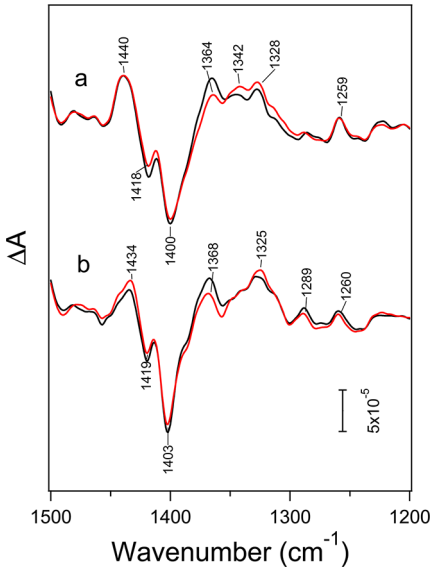

Figure 4. S_2/S_1 FTIR difference spectra in the 1500−1200 cm^{-1} region of the $^{15}NO_3^-$-treated PSII complexes (red lines) from WT (a) and D2-K317R (b) in comparison with those of $^{14}NO_3^-$-treated PSII (black lines, Figure 3).

NO_3^- region of the $^{15}NO_3^-$-treated and $^{14}NO_3^-$ (natural abundance)-treated PSII core complexes (red and black lines, respectively) of WT (a) and K317R (b). Small but clear differences were observed around 1350 cm^{-1}.

Isotope-edited NO_3^- bands without protein contributions were obtained in the $^{14}NO_3^-$-minus-$^{15}NO_3^-$ double difference spectra (Figure 5). The spectrum of WT (Figure 5a) showed a large positive peak at 1368 cm^{-1} concomitant with a negative peak at 1417 cm^{-1}, a broad negative signal at ∼1320 cm^{-1}, and a positive signal at 1279 cm^{-1}. These features were similar to the previously reported $^{14}NO_3^-$-minus-$^{15}NO_3^-$ double difference spectra of the PSII membranes[42] and PSII core complexes[43] from spinach, in which bands were observed at 1406, 1369, 1323, and 1288 cm^{-1} and at 1415, 1369, 1319, and 1284 cm^{-1}, respectively.

Similar band features were also observed at 1430, 1265, 1324, and 1285 cm^{-1} in the $^{14}NO_3^-$-minus-$^{15}NO_3^-$ double difference spectrum of D2-K317R (Figure 5b). The signal intensities were also similar to those of WT (Figure 5a), indicating that the Cl^- ion(s) at the same site(s) as WT was replaced with NO_3^- in D2-K317R. The random noise levels of these spectra are shown

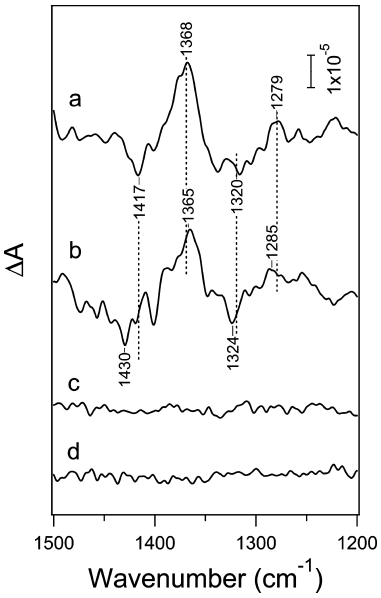

Figure 5. $^{14}NO_3^-$-minus-$^{15}NO_3^-$ double difference spectra of the S_2/S_1 difference spectra of the NO_3^--treated PSII complexes from WT (a) and D2-K317R (b) and double difference spectra of the dark-minus-dark spectra of WT (c) and D2-K317R (d) representing noise levels.

in the corresponding double difference spectra of the dark-minus-dark spectra of WT (Figure 5c) and D2-K317R (Figure 5d). It is clear that the negative peak at 1417 cm^{-1} in WT is upshifted to 1430 cm^{-1} in D2-K317R. The strongest peak at 1368 cm^{-1} and the positive peak at 1279 cm^{-1} seem to be slightly downshifted and upshifted to 1365 and 1285 cm^{-1}, respectively, by the D2-K317R mutation. The broad feature at ∼1320 cm^{-1} in WT was changed to a relatively sharp peak at 1324 cm^{-1} in K317R.

Figure 6 shows the FTIR difference spectra of the S-state cycle obtained by applying four flashes on the hydrated films of WT (black lines) and D2-K317R (red line). The spectral features of WT were very similar to those reported previously.[35−37] In particular, the spectral intensities of the individual S-state transitions were comparable to those by Debus and colleagues.[36,55] The effects of the mutation on the first-flash spectrum were similar to those of the S_2/S_1 spectrum in Figure 2, e.g., slight upshifts of the peaks at 1416, 1398, and 1364 cm^{-1} to 1418, 1402, and 1366 cm^{-1}, respectively, in the symmetric COO^- region and decreases in intensities of the 1588, 1543, and 1523 cm^{-1} peaks in the asymmetric COO^-/amide II region. The change of the negative COOH band at 1747 cm^{-1} to a positive band at 1744 cm^{-1} was also similar to Figure 2. However, some differences were detected especially in the amide I region; the intensity increases at 1619 and 1674 cm^{-1} in Figure 2 were not detected in Figure 6a. This could be due to subtle changes in the sample conditions, such as the extent of hydration, that affect the intensities of the amide I bands.

The features of the second-flash spectra, which mostly represent the $S_2 \rightarrow S_3$ transition, were similar between WT and D2-K317R especially in the symmetric COO^- region (1450−1300 cm^{-1}) except for small frequency shifts (from 1445 to 1443 cm^{-1} and from 1395 to 1399 cm^{-1}, respectively) (Figure 6b). However, the features of the asymmetric COO^-/amide II region at 1600−1500 cm^{-1} were rather different, e.g., the appearance of a negative peak at 1543 cm^{-1} and the decrease

dx.doi.org/10.1021/bi301699h | Biochemistry 2013, 52, 4748−4757

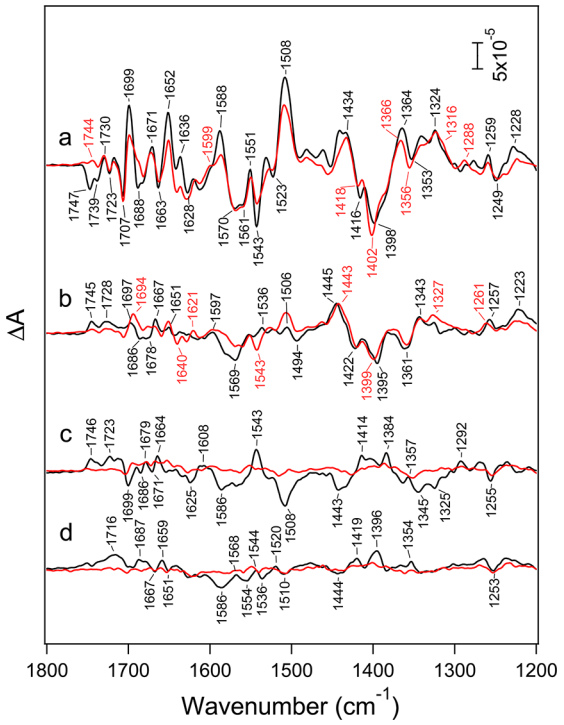

Figure 6. Flash-induced FTIR difference spectra of the S-state cycle in moderately hydrated films of PSII complexes from WT (black lines) and D2-K317R (red lines): (a) first flash, (b) second flash, (c) third flash, and (d) fourth flash.

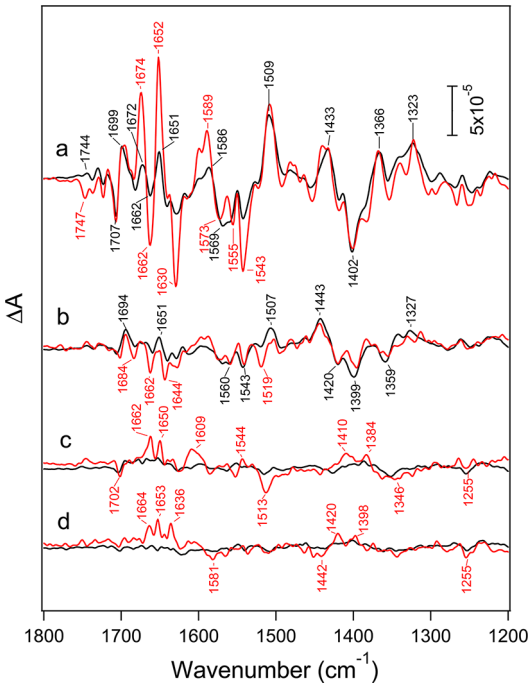

Figure 7. Flash-induced FTIR difference spectra of the S-state cycle of PSII complexes from D2-K317R in a buffer solution (red lines) in comparison with those in a moderately hydrated film (black line): (a) first flash, (b) second flash, (c) third flash, and (d) fourth flash.

and increase in the intensity of the 1569 and 1506 cm^{-1} bands, respectively. These changes following the second flash in the D2-K317R mutant were similar to those in FTIR spectra of several mutants of carboxylate residues around the Mn_4CaO_5 cluster detected by Service et al.[55]

It is notable that the overall spectral intensities significantly decreased and band features almost disappeared by mutation at the third- and fourth-flash spectra. This can be ascribed to a significant decrease in the efficiency of the $S_3 \rightarrow S_0$ transition of the D2-K317R core complexes because of partial dehydration of the PSII protein in the moderately hydrated film used for the experiments.

To confirm this idea, an FTIR spectrum of the S-state cycle was measured using a solution sample of D2-K317R (Figure 7, red line). In the third-flash spectrum (Figure 7c, red line), peaks at 1702, 1609, 1544, 1513, 1410, 1384, and 1346 cm^{-1} corresponding to the peaks at 1699, 1608, 1543, 1508, 1414, 1384, and 1345 cm^{-1}, respectively, in the third-flash spectrum of WT (Figure 6c, black line) were clearly shown. Also, in the fourth-flash spectrum (Figure 7d, red line), peaks at 1581, 1442, 1420, 1398, and 1255 cm^{-1} corresponding to the peaks at 1586, 1444, 1419, 1396, and 1253 cm^{-1}, respectively, in the fourth-flash spectrum of WT (Figure 6d, black line) were observed. These observations indicate that the $S_3 \rightarrow S_0$ transition as well as the $S_0 \rightarrow S_1$ transition is not blocked in the D2-K317R mutant in solution. The spectral similarities suggest that there are no drastic structural changes in the $S_3 \rightarrow S_0$ and $S_0 \rightarrow S_1$ transitions between D2-K317R and WT. Furthermore, it is notable that the negative COOH band at 1748 cm^{-1}, which was observed in the S_2/S_1 spectrum of WT but was absent in the spectrum of the hydrated film of K317R (Figure 1a, b), appeared in the first-flash spectrum of the solution sample of this mutant (Figure 7a, red line). Another characteristic of the solution spectra is stronger features in the amide I region (1700−1600 cm^{-1}), indicative of more flexible movements of the protein main chains around the Mn_4CaO_5 cluster in solution than in a hydrated film.

DISCUSSION

The side chain of D2-K317 interacts with one of the two Cl^- ions, Cl-1, in the high-resolution (1.9 Å) X-ray structure of PSII.[9] Cl-1 is linked with the Mn_4CaO_5 cluster through the backbone NH group of D1-E333, a bridging ligand to Mn2 and Mn4, and also through a hydrogen bond network that includes water molecules and D1-D61 (Figure 1). These water molecules in the network involve W1 and W2, which are the direct ligands to Mn4 and candidates for substrate water. Thus, it is expected that the impact of the mutation of D2-K317 provides insight into the structural coupling of Cl-1 with the Mn_4CaO_5 cluster and its role in the water oxidation reaction.

The D2-K317R mutant retained O_2 evolution activity [2000−2900 μmol of O_2 (mg of Chl)$^{-1}$ h^{-1}] as well as basic features of the S_2/S_1 FTIR difference spectrum (Figure 2), suggesting that no serious alterations took place in the structure of the Mn_4CaO_5 cluster. These observations also provide evidence that Cl^- is basically retained in the WOC of the D2-K317R mutant, because Cl^- depletion inhibits O_2 evolution,[15−17] and the previous FTIR spectrum of Cl^--depleted PSII showed a much weaker intensity in the symmetric COO^- band at ∼1400 cm^{-1}.[42] Although the spectra are broadly similar, the D2-K317R mutation did, however, induce some clear differences in the S_2/S_1 FTIR spectrum in the symmetric COO^- stretching (1450−1300 cm^{-1}), asymmetric COO^- stretching/amide II (1600−1500 cm^{-1}), amide I (1700−1600 cm^{-1}), and COOH (1750−1700 cm^{-1}) regions (Figure 2). This indicates that D2-K317 is structurally coupled with the Mn_4CaO_5 cluster, even though it is ∼7 Å from the nearest Mn

dx.doi.org/10.1021/bi301699h | Biochemistry 2013, 52, 4748−4757

ion (Mn4), and that the mutation perturbs the COO^-/COOH groups and protein conformations that undergo structural changes upon the $S_1 \rightarrow S_2$ transition.

The WT-minus-K317R double difference spectrum (Figure 2c) showed peaks at 1443, 1417, and 1407, 1394, and 1362 cm^{-1} in the symmetric COO^- stretching region. The primary candidates for the carboxylate groups responsible for these peaks are those of D1-E333 and D1-D61 because of the putative interactions with D2-K317 through Cl-1 and/or water molecules as mentioned above. Previous FTIR measurements of the D1-D61A mutant,[55] however, did not show drastic changes in the symmetric COO^- region of the S_2/S_1 difference spectrum. The peak at 1394 cm^{-1} agrees with that of CP43-E354 in the S_1 state, which has been identified using the CP43-E354Q mutant.[36,37] However, the corresponding band in the S_2 state at 1431 cm^{-1} in the previous study[36,37] was not observed in this study. The COO^- signal as a counterpart of the negative COOH peak at 1749 cm^{-1} (see below) should appear in this COO^- region. However, the spectrum of NO_3^--treated PSII, which did not show this negative COOH signal, also provided similar double difference signals at 1442, 1416, 1405, 1392, and 1360 cm^{-1} in the COO^- region (Figure 3c), indicating the contribution of this deprotonation reaction to the COO^- signals is not large. Thus, at present, it is difficult to assign the COO^- signals affected by the D2-K317R mutation to specific carboxylate residues.

The coupling of the Cl-1 site with the Mn_4CaO_5 cluster was more directly examined by NO_3^- replacement of Cl^- in WT and D2-K317R. By taking a double difference between the spectra of the $^{15}NO_3^-$- and $^{14}NO_3^-$-treated samples, one can abstract only the vibrations of NO_3^- ions coupled to the Mn_4CaO_5 cluster.[42,43] Furthermore, via examination of the effect of the D2-K317R mutation, the interaction of the NO_3^- bound to the Cl-1 site can be specifically studied. Hasegawa et al.[43] previously showed using spinach PSII that NO_3^- replacing Cl^- near the Mn_4CaO_5 cluster has asymmetric NO stretching bands only at 1450−1250 cm^{-1}, which provided evidence that the NO_3^- is free from metal binding. From careful analysis of the $^{14}NO_3^-$-minus-$^{15}NO_3^-$ and $N^{16}O_3^-$-minus-$N^{18}O_3^-$ signals, they concluded that NO_3^- has a rather asymmetric structure in the S_1 state showing split bands at 1415 and ∼1320 cm^{-1}, while it has a more symmetric structure in the S_2 state showing a band at ∼1370 cm^{-1}.[43]

Our $^{14}NO_3^-$-minus-$^{15}NO_3^-$ S_2/S_1 double difference spectrum of PSII from WT *Synechocystis* in moderately hydrated films at 283 K (Figure 5a) showed band features at 1417, 1368, 1320, and 1279 cm^{-1} similar to those of spinach PSII (1406, 1369, 1323, and 1288 cm^{-1} and 1415, 1369, 1319, and 1284 cm^{-1} for PSII membranes and core complexes, respectively) in the pellet forms at 250 K, indicating that the interaction of NO_3^- at the Cl^- site(s) is very similar between higher plants and cyanobacteria. Also, the sample forms (moderately hydrated films vs pellets) and temperatures (283 K vs 250 K) are not related to the frequencies of NO_3^- bands. In the D2-K317R mutant, the band pattern and intensities of the NO_3^- signals did not change significantly (Figure 5b), consistent with similar binding of NO_3^- in the WT and mutant. Upon closer inspection, however, it is clearly seen that the highest-frequency peak at 1417 cm^{-1} is upshifted to 1430 cm^{-1}. Also, a rather broad feature around 1320 cm^{-1} became sharper with a peak at 1324 cm^{-1} and positive peaks at 1368 and 1279 cm^{-1} slightly downshift and upshift to 1365 and 1285 cm^{-1}, respectively. Because it is highly expected that the D2-K317R mutation predominantly perturbs the NO_3^- at the Cl-1 site, these changes indicate that the observed NO_3^- bands contains the vibrations of NO_3^- at the Cl-1 site. This also indicates that the NO_3^- at the Cl-1 site, and thus probably the Cl^- ion at this site in untreated PSII, has a specific structural coupling with the Mn_4CaO_5 cluster and the interaction is perturbed upon formation of S_2. It is likely that the observed NO_3^- signals are the result of the overlap of the bands of NO_3^- at the Cl-1 and Cl-2 sites, although further investigation is necessary to prove the involvement of the NO_3^- signal at the Cl-2 site.

On the basis of the assignments of the NO_3^- bands by Hasegawa et al.,[42,43] the highest-frequency peak at 1417 cm^{-1} can be assigned to one of the split NO stretching vibrations of $^{14}NO_3^-$ with an asymmetric structure in the S_1 state, while the lowest-frequency peak at 1279 cm^{-1} can be assigned to the other NO stretching vibration of $^{15}NO_3^-$. A large upshift of the former peak by ∼13 cm^{-1} and a smaller upshift of the latter by ∼6 cm^{-1} imply a larger split of the asymmetric NO stretching vibrations with an upshift of the center of the frequency gap. This observation suggests that NO_3^- at the Cl-1 site in the S_1 state has a more asymmetric interaction and weaker hydrogen bonding in the D2- K317R mutant than in WT. This change may be caused by the changes in the hydrogen bond properties (e.g., acidity of the NH group, distance, and angle) and the electrostatic interaction (a positive charge is more distributed over the side chain in Arg than Lys) by the Lys to Arg mutation. The change in the interaction of chloride in the Cl-1 site by this mutation is consistent with the observation that the O_2 evolution activity of the core complexes at relatively low Cl^- concentrations (<10 mM) is lower for the D2-K317R mutant than for WT [Figure S3 of the Supporting Information; also consistent data were observed by Pokhrel et al.[49]], suggestive of the reduced binding affinity of Cl^-. The biphasic curves in Figure S3 of the Supporting Information could be due to the minor heterogeneity in the preparations. This susceptibility to Cl^- of the isolated core complexes, however, did not provide a drastic effect *in vivo* as shown in the similar growth curves between D2-K317R and WT even in the medium depleted of Cl^- (Figure S2 of the Supporting Information).

The involvement of a COOH/COO^- group(s) in the hydrogen bond network around D2-K317 and Cl-1 was also revealed by the change in the C═O stretching band of COOH at 1750−1740 cm^{-1}; the negative peak at 1748 cm^{-1} in the untreated PSII from WT was changed to a positive peak at 1742−1743 cm^{-1} by both the D2-K317R mutation and NO_3^- treatment upon examination in moderately hydrated films (Figures 2 and 3). It is presumed that the D2-K317R mutation and the Cl^- to NO_3^- change affected the pK_a of a nearby COOH/COO^- group(s) though a hydrogen bond network. Service et al.[55] previously observed very similar effects on the COOH bands by D1-E65A, D2-E312A, and D1-E329A mutations and concluded that these residues are in a common network of hydrogen bonds that includes water molecules and carboxylate groups and mutation of any of these residues disrupts the network. Indeed, the X-ray structure[9] showed that D1-E65 and D2-E312 are located near D2-K317 with distances of 4−6 Å and mutually related through a hydrogen bond network that includes water molecules (Figure 1). Thus, it is logical that D2-K317 is also involved in the same hydrogen bond network affecting the pK_a of a COOH group(s) upon the $S_1 \rightarrow S_2$ transition. The involvement of water molecules in this hydrogen bond network was revealed by the recovery of the negative COOH band at 1748 cm^{-1} when the D2-K317R

dx.doi.org/10.1021/bi301699h | *Biochemistry* 2013, 52, 4748−4757

mutant was examined in solution rather than in film (Figure 7a). The decrease in the intensity of the 1748 cm^{-1} band by dehydration of the sample was previously reported by Service et al.[55] in the PSII core complexes of WT *Synechocystis*. Our observation of the absence of this band in the hydrated film of the D2-K317R mutant formed at a relative humidity of 95% (by 40% glycerol/water)[50] despite the presence of the band in the same hydrated film of WT indicates that sensitivity to dehydration is increased by this mutation. These results are consistent with the view that the carboxylate groups showing the 1748 cm^{-1} band, D2-K317, and water molecules, some of which are deleted by partial dehydration, are connected through a common hydrogen bond network.

The carboxylate residue responsible for the negative peak at 1748 cm^{-1} has not yet been identified.[55] It could arise from several carboxylate groups involved in the hydrogen bond network rather than one specific residue. This view is consistent with the fact that a specific peak of the symmetric COO^- vibration coupled with the COOH band at 1748 cm^{-1} was not clearly identified in the 1450−1300 cm^{-1} region (see above). Although the carboxylate group of D1-E329 is ∼15−20 Å from D2-K317, D1-E65, and D2-E312, Service et al.[55] suggested that the postulated network extends for at least 20 Å.

FTIR spectra of the S-state cycle (Figure 6) showed that the efficiency of the $S_3 \rightarrow S_0$ transition significantly decreased in the moderately hydrated film of the D2-K317R mutant. Because the PSII core complexes from the D2-K317R mutant retained a relatively high O_2 evolution rate [2000−2900 μmol of O_2 (mg of Chl)$^{-1}$ h^{-1}] and the FTIR spectra in the solution sample of the K317R mutant exhibited better S-state cycling (Figure 7), this observation indicates that the sensitivity of the $S_3 \rightarrow S_0$ transition to sample dehydration is increased by the K317R mutation. The FTIR spectra of Pokhrel et al.[49] of the hydrated film of D2-K317R were very similar to our solution spectra of the same mutant (Figure 7), probably because of a higher extent of hydration, which is determined by the ratio of a glycerol/water solution enclosed in the sample cell [20% (v/v) glycerol/water in the work of Pokhrel et al.[49] vs 40% in our experiment].[50] Service et al.[55] also observed a decrease in the $S_3 \rightarrow S_0$ efficiency caused by D1-D61A, D1-E65A, and D2-E312A mutations and suggested the participation of these residues in a proton egress channel from the Mn_4CaO_5 cluster to the lumen. These carboxylate residues are all located near D2-K317 and connected through hydrogen bonds (Figure 1). Thus, together with a hydrogen bond network involving D2-K317 that affects pK_a values of $COOH/COO^-$ groups, the observation of the decrease in the efficiency of the $S_3 \rightarrow S_0$ transition suggests that D2-K317 and the Cl-1 site are also involved in the same proton pathway as D1-D61, D1-E65, and D2-E312. The involvement of Cl-1 in a proton pathway is consistent with the recent molecular dynamics and Monte Carlo simulation, in which depletion of Cl-1 induces formation of a salt bridge between D2-K317 and D1-D61 that suppresses the proton transfer.[26] The X-ray structure at 1.9 Å resolution[9] detected many water molecules in this putative pathway. Thus, it is presumed that the effect of mutation, which slightly altered the hydrogen bond network in the proton pathway, was more emphasized by removal of some of these water molecules in partially dehydrated PSII proteins. Proton release is thought to take place in the three transitions other than the $S_1 \rightarrow S_2$ transition.[51,59] Because the efficiency of the $S_2 \rightarrow S_3$ transition was not significantly affected by the K317R mutation (Figure 6) and the $S_0 \rightarrow S_1$ transition is proposed to be unaffected by Cl^- depletion,[17] it is possible that the proton pathway involving Cl-1 functions mainly in the $S_3 \rightarrow S_0$ transition. The role of Cl^- in the proton pathway in the $S_3 \rightarrow S_0$ transition is consistent with the previous time-resolved UV absorption studies, in which replacement of Cl^- with other functional monovalent ions retards the rate of the $S_3 \rightarrow S_0$ transition.[18,19]

Broser et al.[25] recently found another Cl^- site (Cl-1B) in the vicinity of Cl-1 (Cl-1A) but distinct from the Cl-2 site in the X-ray structure (3.2 Å resolution) of terbutryn-bound PSII core complexes. The Cl-1B site exhibited an even higher occupancy (∼70%) than Cl-1A (∼30%). The Cl-1B site also interacts with the side chain of D2-K317 along with the side chains of D1-R334 and D1-N335. Thus, we cannot fully exclude the possibility that our observation of the effect of the D2-K317R mutation is actually related to Cl-1B, which could be moved from the Cl-1A site during the S-state cycle[25] or by some other condition.

In conclusion, FTIR measurements of the D2-K317R mutant in combination with Cl^-/NO_3^- replacement have provided experimental evidence that the Cl-1 site is structurally coupled with the Mn_4CaO_5 cluster and that the D2-K317R mutation perturbs the changes in protein structure induced by formation of the S_2 state. This is consistent with the previous FTIR studies that showed significant FTIR changes by Cl^- depletion or replacement of Cl^- with nonfunctional univalent anions such as F^- and acetate.[42] However, this work is the first to show a specific interaction of Cl-1 with the WOC. One of the roles of Cl-1 may be to stabilize the structure of the WOC through interactions with the protein backbone connecting two ligands (D1-E333 and D1-H332) to the Mn_4CaO_5 cluster, thereby preserving a rigid hydrogen bond network around the WOC. It was also shown that the hydrogen bond network involving D2-K317 and Cl-1 controls the pK_a of $COOH/COO^-$ groups coupled to the Mn_4CaO_5 cluster. The presence of this hydrogen bond network and the decrease in the efficiency of the $S_3 \rightarrow S_0$ transition by partial dehydration of the D2-K317R mutant suggest that D2-K317 and Cl-1 are involved in the proton transfer pathway from the Mn_4CaO_5 cluster to the lumen, which functions mainly in the $S_3 \rightarrow S_0$ transition. It is also possible that structural changes in the Mn_4CaO_5 cluster during the S-state cycle are relayed to Cl-1 through the D1-E333 and D1-H332 ligands, thereby changing the structure and activity of the proton channel, to gate proton transfer.

■ ASSOCIATED CONTENT

Supporting Information

Diagram of the measurement procedure for FTIR difference spectra of the $S_1 \rightarrow S_2$ transition and the S-state cycle, growth curves for D2-K317R and the WT control, and Cl^- concentration dependence of the O_2 evolution activities of the PSII core complexes. This material is available free of charge via the Internet at http://pubs.acs.org.

■ AUTHOR INFORMATION

Corresponding Author

*E-mail: tnoguchi@bio.phys.nagoya-u.ac.jp. Phone: (+81)52-789-2881.

Author Contributions

H.S. and J.Y. are joint first authors.

Funding

This study was supported by the Grants-in-Aid for Scientific Research from the Ministry of Education, Culture, Sports,

Science and Technology (23657099, 24000018, 24107003, and 25291033) to T.N. and the Biotechnology and Biological Sciences Research Council (BB/C507037) to P.J.N.

Notes

The authors declare no competing financial interest.

■ ACKNOWLEDGMENTS

We thank Professor Gary Brudvig and his co-workers for communicating their results in advance and Alina Huth for help with the growth experiments.

■ ABBREVIATIONS

DM, *n*-dodecyl β-D-maltoside; FTIR, Fourier transform infrared; Mes, 2-(*N*-morpholino)ethanesulfonic acid; PSII, photosystem II; $(S_3Y_Z^{\bullet})'$, intermediate before electron transfer from the Mn_4CaO_5 cluster to $Y_Z^{\bullet}$ in the $S_3 \rightarrow S_0$ transition; WOC, water-oxidizing center; WT, wild type.

■ REFERENCES

(1) Debus, R. J. (1992) The manganese and calcium ions of photosynthetic oxygen evolution. *Biochim. Biophys. Acta 1102*, 269−352.

(2) Hillier, W., and Messinger, J. (2005) Mechanism of photosynthetic oxygen production. In *Photosystem II: The Light-Driven Water:Plastoquinone Oxidoreductase* (Wydrzynski, T., and Satoh, K., Eds.) pp 567−608, Springer, Dordrecht, The Netherlands.

(3) McEvoy, J. P., and Brudvig, G. W. (2006) Water-splitting chemistry of photosystem II. *Chem. Rev. 106*, 4455−4483.

(4) Messinger, J., Noguchi, T., and Yano, J. (2012) Photosynthetic O_2 evolution. In *Molecular Solar Fuels* (Wydrzynski, T., and Hillier, W., Eds.) Chapter 7, pp 163−207, Royal Society of Chemistry, Cambridge, U.K.

(5) Renger, G. (2012) Photosynthetic water splitting: Apparatus and mechanism. In *Photosynthesis: Plastid Biology, Energy Conversion and Carbon Assimilation* (Eaton-Rye, J. J., Tripathy, B. C., and Sharkey, T. D., Eds.) pp 359−414, Springer, Dordrecht, The Netherlands.

(6) Grundmeier, A., and Dau, H. (2012) Structural models of the manganese complex of photosystem II and mechanistic implications. *Biochim. Biophys. Acta 1817*, 88−105.

(7) Ferreira, K. N., Iverson, T. M., Maghlaoui, K., Barber, J., and Iwata, S. (2004) Architecture of the photosynthetic oxygen-evolving center. *Science 303*, 1831−1838.

(8) Guskov, A., Kern, J., Gabdulkhakov, A., Broser, M., Zouni, A., and Saenger, W. (2009) Cyanobacterial photosystem II at 2.9-Å resolution and the role of quinones, lipids, channels and chloride. *Nat. Struct. Mol. Biol. 16*, 334−342.

(9) Umena, Y., Kawakami, K., Shen, J. R., and Kamiya, N. (2011) Crystal structure of oxygen-evolving photosystem II at a resolution of 1.9 Å. *Nature 473*, 55−60.

(10) Yano, J., Kern, J., Sauer, K., Latimer, M. J., Pushkar, Y., Biesiadka, J., Loll, B., Saenger, W., Messinger, J., Zouni, A., and Yachandra, V. K. (2006) Where water is oxidized to dioxygen: Structure of the photosynthetic Mn_4Ca cluster. *Science 314*, 821−825.

(11) van Gorkom, H. J., and Yocum, C. F. (2005) The calcium and chloride cofactors. In *Photosystem II: The Light-Driven Water:-Plastoquinone Oxidoreductase* (Wydrzynski, T., and Satoh, K., Eds.) pp 307−327, Springer, Dordrecht, The Netherlands.

(12) Popelkova, H., and Yocum, C. F. (2007) Current status of the role of Cl^- ion in the oxygen-evolving complex. *Photosynth. Res. 93*, 111−121.

(13) Yocum, C. F. (2008) The calcium and chloride requirements of the O_2 evolving complex. *Coord. Chem. Rev. 252*, 296−305.

(14) Pokhrel, R., McConnell, I. L., and Brudvig, G. W. (2011) Chloride regulation of enzyme turnover: Application to the role of chloride in photosystem II. *Biochemistry 50*, 2725−2734.

(15) Ono, T., Zimmermann, J. L., Inoue, Y., and Rutherford, A. W. (1986) EPR evidence for a modified S-state transition in chloride-depleted Photosystem II. *Biochim. Biophys. Acta 851*, 193−201.

(16) Boussac, A., Setif, P., and Rutherford, A. W. (1992) Inhibition of tyrosine Z photooxidation after formation of the S_3 state in calcium-depleted and chloride-depleted photosystem-II. *Biochemistry 31*, 1224−1234.

(17) Wincencjusz, H., van Gorkom, H. J., and Yocum, C. F. (1997) The photosynthetic oxygen evolving complex requires chloride for its redox state $S_2 \rightarrow S_3$ and $S_3 \rightarrow S_0$ transitions but not for $S_0 \rightarrow S_1$ or $S_1 \rightarrow S_2$ transitions. *Biochemistry 36*, 3663−3670.

(18) Wincencjusz, H., Yocum, C. F., and van Gorkom, H. J. (1999) Activating anions that replace Cl^- in the O_2-evolving complex of photosystem II slow the kinetics of the terminal step in water oxidation and destabilize the S_2 and S_3 states. *Biochemistry 38*, 3719−3725.

(19) Boussac, A., Ishida, N., Sugiura, M., and Rappaport, F. (2012) Probing the role of chloride in Photosystem II from *Thermosynechococcus elongatus* by exchanging chloride for iodide. *Biochim. Biophys. Acta 1817*, 802−810.

(20) Lindberg, K., and Andréasson, L. E. (1996) A one-site, two-state model for the binding of anions in photosystem II. *Biochemistry 35*, 14259−14267.

(21) Boussac, A. (1995) Exchange of chloride by bromide in the manganese photosystem II complex studied by cw- and pulsed-EPR. *Chem. Phys. 194*, 409−418.

(22) van Vliet, P., and Rutherford, A. W. (1996) Properties of the chloride-depleted oxygen-evolving complex of photosystem II studied by electron paramagnetic resonance. *Biochemistry 35*, 1829−1839.

(23) Murray, J. W., Maghlaoui, K., Kargul, J., Ishida, N., Lai, T. L., Rutherford, A. W., Sugiura, M., Boussac, A., and Barber, J. (2008) X-ray crystallography identifies two chloride binding sites in the oxygen evolving centre of Photosystem II. *Energy Environ. Sci. 1*, 161−166.

(24) Kawakami, K., Umena, Y., Kamiya, N., and Shen, J. R. (2009) Location of chloride and its possible functions in oxygen-evolving photosystem II revealed by X-ray crystallography. *Proc. Natl. Acad. Sci. U.S.A. 106*, 8567−8572.

(25) Broser, M., Glöckner, C., Gabdulkhakov, A., Guskov, A., Buchta, J., Kern, J., Müh, F., Dau, H., Saenger, W., and Zouni, A. (2011) Structural basis of cyanobacterial photosystem II inhibition by the herbicide terbutryn. *J. Biol. Chem. 286*, 15964−15972.

(26) Rivalta, I., Amin, M., Luber, S., Vassiliev, S., Pokhrel, R., Umena, Y., Kawakami, K., Shen, J. R., Kamiya, N., Bruce, D., Brudvig, G. W., Gunner, M. R., and Batista, V. S. (2011) Structural-functional role of chloride in photosystem II. *Biochemistry 50*, 6312−6315.

(27) Chu, H.-A., Hillier, W., Law, N. A., and Babcock, G. T. (2001) Vibrational spectroscopy of the oxygen-evolving complex and of manganese model compounds. *Biochim. Biophys. Acta 1503*, 69−82.

(28) Noguchi, T., and Berthomieu, C. (2005) Molecular analysis by vibrational spectroscopy. In *Photosystem II: The Light-Driven Water:-Plastoquinone Oxidoreductase* (Wydrzynski, T., and Satoh, K., Eds.) pp 367−387, Springer, Dordrecht, The Netherlands.

(29) Noguchi, T. (2007) Light-induced FTIR difference spectroscopy as a powerful tool toward understanding the molecular mechanism of photosynthetic oxygen evolution. *Photosynth. Res. 91*, 59−69.

(30) Debus, R. J. (2008) Protein ligation of the photosynthetic oxygen-evolving center. *Coord. Chem. Rev. 252*, 244−258.

(31) Noguchi, T. (2008) Fourier transform infrared analysis of the photosynthetic oxygen-evolving center. *Coord. Chem. Rev. 252*, 336−346.

(32) Chu, H.-A., Sackett, H., and Babcock, G. T. (2000) Identification of a Mn-O-Mn cluster vibrational mode of the oxygen-evolving complex in photosystem II by low-frequency FTIR spectroscopy. *Biochemistry 39*, 14371−14376.

(33) Noguchi, T., Ono, T., and Inoue, Y. (1995) Direct detection of a carboxylate bridge between Mn and Ca^{2+} in the photosynthetic oxygen-evolving center by means of Fourier transform infrared spectroscopy. *Biochim. Biophys. Acta 1228*, 189−200.

(34) Chu, H.-A., Hillier, W., and Debus, R. J. (2004) Evidence that the C-terminus of the D1 polypeptide of photosystem II is ligated to the manganese ion that undergoes oxidation during the S_1 to S_2 transition: An isotope-edited FTIR study. *Biochemistry 43*, 3152−3166.
(35) Kimura, Y., Mizusawa, N., Ishii, A., and Ono, T. (2005) FTIR detection of structural changes in a histidine ligand during S-state cycling of photosynthetic oxygen-evolving complex. *Biochemistry 44*, 16072−16078.
(36) Service, R. J., Yano, J., McConnell, I., Hwang, H. J., Niks, D., Hille, R., Wydrzynski, T., Burnap, R. L., Hillier, W., and Debus, R. J. (2011) Participation of glutamate-354 of the CP43 polypeptide in the ligation of manganese and the binding of substrate water in photosystem II. *Biochemistry 50*, 63−81.
(37) Shimada, Y., Suzuki, H., Tsuchiya, T., Tomo, T., Noguchi, T., and Mimuro, M. (2009) Effect of a single amino acid substitution of the 43 kDa chlorophyll-protein on the oxygen-evolving reaction of the cyanobacterium *Synechocystis* sp. PCC 6803: Analysis of the Glu354Gln mutation. *Biochemistry 48*, 6095−6103.
(38) Shimada, Y., Suzuki, H., Tsuchiya, T., Mimuro, M., and Noguchi, T. (2011) Structural coupling of an arginine side chain with the oxygen evolving Mn_4Ca cluster in photosynstem II as revealed by isotope-edited Fourier transform infrared spectroscopy. *J. Am. Chem. Soc. 133*, 3808−3811.
(39) Tomita, M., Ifuku, K., Sato, F., and Noguchi, T. (2009) FTIR evidence that the PsbP extrinsic protein induces protein conformational changes around the oxygen-evolving Mn cluster in photosystem II. *Biochemistry 48*, 6318−6325.
(40) Noguchi, T., and Sugiura, M. (2002) FTIR detection of water reactions during the flash-induced S-state cycle of the photosynthetic water-oxidizing complex. *Biochemistry 41*, 15706−15712.
(41) Suzuki, H., Sugiura, M., and Noguchi, T. (2008) Monitoring water reactions during the S-state cycle of the photosynthetic water-oxidizing center: Detection of the DOD bending vibrations by means of Fourier transform infrared spectroscopy. *Biochemistry 47*, 11024−11030.
(42) Hasegawa, K., Kimura, Y., and Ono, T. (2002) Chloride cofactor in the photosynthetic oxygen-evolving complex studied by Fourier transform infrared spectroscopy. *Biochemistry 41*, 13839−13850.
(43) Hasegawa, K., Kimura, Y., and Ono, T. (2004) Oxidation of the Mn cluster induces structural changes of NO_3^- functionally bound to the Cl^- site in the oxygen-evolving complex of photosystem II. *Biophys. J. 86*, 1042−1050.
(44) Tang, X. S., Chisholm, D. A., Dismukes, G. C., Brudvig, G. W., and Diner, B. A. (1993) Spectroscopic evidence from site-directed mutants of *Synechocystis* PCC6803 in favor of a close interaction between histidine 189 and redox-active tyrosine 160, both of polypeptide D2 of the photosystem II reaction center. *Biochemistry 32*, 13742−13748.
(45) Boehm, M., Romero, E., Reisinger, V., Yu, J., Komenda, J., Eichacker, L. A., Dekker, J. P., and Nixon, P. J. (2011) Investigating the early stages of photosystem II assembly in *Synechocystis* sp. PCC 6803. *J. Biol. Chem. 286*, 14812−14819.
(46) Bricker, T. M., Morvant, J., Masri, N., Sutton, H. M., and Frankel, L. K. (1990) Isolation of a highly active Photosystem II preparation from *Synechocystis* 6803 using a histidine-tagged mutant of CP 47. *Biochim. Biophys. Acta 1409*, 50−57.
(47) Noren, G. H., Boerner, R. J., and Barry, B. A. (1991) EPR characterization of an oxygen-evolving photosystem II preparation from the transformable cyanobacterium *Synechocystis* 6803. *Biochemistry 30*, 3943−3950.
(48) Tang, X.-S., and Diner, B. A. (1994) Biochemical and spectroscopic characterization of a new oxygen-evolving photosystem II core complex from the cyanobacterium *Synechocystis* PCC 6803. *Biochemistry 33*, 4594−4603.
(49) Pokhrel, R., Service, R. J., Debus, R. J., and Brudvig, G. W. (2013) Mutation of lysine 317 in the D2 subunit of photosystem II alters chloride binding and proton transport. *Biochemistry*, DOI: 10.1021/bi301700u.
(50) Noguchi, T., and Sugiura, M. (2002) Flash-induced FTIR difference spectra of the water oxidizing complex in moderately hydrated photosystem II core films: Effect of hydration extent on S-state transitions. *Biochemistry 41*, 2322−2330.
(51) Suzuki, H., Sugiura, M., and Noguchi, T. (2009) Monitoring proton release during photosynthetic water oxidation in photosystem II by means of isotope-edited infrared spectroscopy. *J. Am. Chem. Soc. 131*, 7849−7857.
(52) Rögner, M., Nixon, P. J., and Diner, B. A. (1990) Purification and characterization of photosystem I and photosystem II core complexes from wild-type and phycocyanin-deficient strains of the cyanobacterium *Synechocystis* PCC 6803. *J. Biol. Chem. 265*, 6189−6196.
(53) Noguchi, T., and Sugiura, M. (2003) Analysis of flash-induced FTIR difference spectra of the S-state cycle in the photosynthetic water-oxidizing complex by uniform ^{15}N and ^{13}C isotope labeling. *Biochemistry 42*, 6035−6042.
(54) Kimura, Y., Mizusawa, N., Ishii, A., Yamanari, T., and Ono, T. (2003) Changes of low-frequency vibrational modes induced by universal ^{15}N- and ^{13}C-isotope labeling in S_2/S_1 FTIR difference spectrum of oxygen-evolving complex. *Biochemistry 42*, 13170−13177.
(55) Service, R. J., Hillier, W., and Debus, R. J. (2010) Evidence from FTIR difference spectroscopy of an extensive network of hydrogen bonds near the oxygen-evolving Mn_4Ca cluster of photosystem II involving D1-Glu65, D2-Glu312, and D1-Glu329. *Biochemistry 49*, 6655−6669.
(56) Hienerwadel, R., Boussac, A., Breton, J., Diner, B. A., and Berthomieu, C. (1997) Fourier transform infrared difference spectroscopy of photosystem II tyrosine D using site-directed mutagenesis and specific isotope labeling. *Biochemistry 36*, 14712−14723.
(57) Takahashi, R., Sugiura, M., and Noguchi, T. (2007) Water molecules coupled to the redox-active tyrosine Y_D in photosystem II as detected by FTIR spectroscopy. *Biochemistry 46*, 14245−14249.
(58) Berthomieu, C., Hienerwadel, R., Boussac, A., Breton, J., and Diner, B. A. (1998) Hydrogen bonding of redox-active tyrosine Z of photosystem II probed by FTIR difference spectroscopy. *Biochemistry 37*, 10547−10554.
(59) Schlodder, E., and Witt, H. T. (1999) Stoichiometry of proton release from the catalytic center in photosynthetic water oxidation: Reexamination by a glass electrode study at pH 5.5−7.2. *J. Biol. Chem. 274*, 30387−30392.